Vol. 3, Iss. 3 (2026) 116-126, DOI: 10.61552/JMES.2026.03.002

Journal of Management and Engineering Sciences

www.jmes.aspur.rs

Mechanical and Fracture Behavior of Various Levels Tin-Doped Copper from Lead-Free Solder Joints Subjected to Thermal Aging

Mohammad Salim Kaiser[a,*]

[a] *Innovation Centre, International University of Business Agriculture and Technology, Dhaka, Bangladesh.*

Keywords:

Scrap copper
Tin
Lead-free solder
Mechanical properties
Fracture behavior
Microstructure
Thermal aging

* Corresponding author:

Mohammad Salim Kaiser
E-mail:
dkaiser.res@iubat.edu

Received: 01.04.2026.
Revised: 03.05.2026.
Accepted: 09.05.2026.

A B S T R A C T

Pure copper may be influenced by contamination from tin, which is frequently introduced during the melting or recycling of scrap material derived from lead-free solder. The research examines the effects of two different levels of tin on waste copper sourced from tin-based lead-free solder. Scrap copper is cleaned by cutting out the major solder joint and using mechanical wire brushing for other portions. Then the cast samples are plastically deformed up to 80% and isochronally aged for 1h at temperatures up to 500°C to analyze stress-strain behavior, hardness, toughness, microstructure, and fracture mode. Results reveal that recycled copper has a tin content of approximately 0.26% to 0.57%, depending on the cleaning process. It improves the alloy's tensile characteristics with the expenses of ductility particularly at lower temperatures for ageing, but is insufficiently beneficial at elevated ageing temperatures. Tin is enhanced through solid solution strengthening and establishes intermetallic bonds with copper and impurities in cast alloys, which obstructs dislocation movement, thereby increasing strength and affecting ductility during the ageing process. The coarsening of precipitates at elevated temperatures diminishes effectiveness, resulting in reduced strength. Rigid intermetallic phases induce crack formation within the matrix, as observed on the fracture surface.

1. INTRODUCTION

Copper is widely used in various industries due to its unique qualities, particularly its excellent electrical and thermal conductivity [1-3]. The need for soldering copper components in applications like heat exchangers, electrical wiring, and circuit boards is crucial. Traditionally, solder contained lead and tin, but there is now a push to find lead-free alternatives to address environmental and health concerns [4].

On the other hand, because environmental preservation is becoming more and more

important, significant attention has been paid to the matter of lead toxicity. Most countries have gradually enacted laws prohibiting the use of lead in solder. These initiatives represent a highly encouraging framework for the advancement and development of innovative soldering materials that are entirely free from lead. Specifically, lead-free tin-based solders, encompassing formulations such as tin-silver, tin-bismuth, tin-copper, tin-indium, tin-antimony, and tin-zinc, have emerged as competitive and viable alternatives to traditional tin-lead solders. Among these, the Sn-Ag-Cu alloy, more commonly identified as SAC305 solder when in its eutectic composition, has gained wide acceptance as the contemporary industry standard due to its reliable performance across a broad spectrum of applications. Furthermore, with the transition to lead-free solders in electronic packaging, Sn-Cu-based variants have garnered significant attention and traction within the industry. This is largely attributed to their exceptional balance of performance characteristics paired with cost-effectiveness. Of particular note, Sn-0.7Cu solders stand out as both an economical option and a promising candidate within the array of newly introduced lead-free alloy systems [5]. A more sustainable society, growing economies, and an aging global population have all contributed to a sharp increase in demand for copper in recent years. The growing need for primary copper can be clarified by that the growth in copper demand is greater than the growth in copper supply from secondary resources. Thus, there is a continuous need for the potential to use old or scrap copper items. However, the user speculates about the deterioration of necessary properties because the scraped copper contains trace amounts of tin, a solder element [6].

It should be mentioned that in its pure form, the strength is somewhat modest, but it can be strengthened through cold working; for alloys, this can be accomplished through cold working, precipitation hardening, and grain refinement, among other conventional methods [6, 7]. Once again, it is worthy of being noted that incorporating additional elements into an alloy can improve certain properties while having different impacts on others. A wide range of literary works provides valuable insights into the impact of alloying various substances with copper. Specifically, when copper is alloyed with tin, it experiences a reduction in conductivity and ductility, while exhibiting improvements in precipitation hardening and overall strength [8]. The addition of Al decreases the corrosion properties despite the similar behavior [9]. Compared to other Cu alloys, silicon is less corrosion-resistant though it increases tensile strength and machinability [10]. Ni-added alloys can maintain their mechanical properties at high temperatures because of their remarkable thermal stability. As previously noted, their extreme hardness results in poor machinability [11, 12]. Once more, the alloy's grain structure and thermal stability are improved by the trace quantity of Zr, and precipitation strengthening is also provided by the addition of Sc [7].

To challenge the skeptic's perspective and investigate the potential of repurposing scrap copper for the creation of new components, it becomes essential to study the behavior of Sn-doped Cu and analyze its various properties in detail. The failure of materials to fracture is a very complex micromechanical process. Against this background, a small number of properties with high Sn content were investigated and interesting results were found regarding the electromechanical behavior, sliding friction, and corrosion behavior of copper scrap when exposed to solder. Experimental research is needed to study the physical and mechanical including stress-strain behavior of scraped Cu under severe plastic deformation and thermal aging for engineering applications. Pure copper and two tin-affected scraped copper variations were used in this context.

2. MATERIALS AND METHODS

2.1 Preparation of the Alloys

Initially, heat exchanger pipes and copper wires were sourced from industrial facilities, recycling centers, and other specific environments, featuring lead-free soldered connections. A section of the scraped copper was used to cut out the major solder joint, while the remaining portion was cleaned with mechanical wire brushing and then given a kerosene wash. Two portions of material are melted conventionally in a clay-graphite crucible with a suitable flux cover known as CERAFLUX-49, using a pit furnace fueled by natural gas. A stable final temperature of 1300±15°C was maintained for the melts. A

mild steel mold that could be adjusted was used. The 20 x 150 x 300 mm mold was carefully adjusted, heated to 250°C, and covered with a layer of clay film. Mechanical mixing was conducted for approximately 5 minutes at a stirring speed of 300 rpm. Following the homogenization of the melts at 1200°C, they were subsequently poured into the heated mold. To prevent excessive gas formation, the furnace temperature is maintained at 1300°C, slightly above the copper's melting temperature of 1085°C, while the pouring temperature is set to 1200°C. One 20 x 150 x 300 mm piece is made per sample. It has been observed that two cast samples contain different amounts of Sn along with trace amounts of other elements with copper. To ascertain the specific effects of Sn, another sample of market available pure copper of 99.99% purity is considered. The chemical compositions, expressed as weight percentages for three materials, were analyzed using the spectrometer Shimadzu PDA 700, as summarized in Table 1.

Table 1. The compositions of the samples.

Alloy	Cu	Sn	Pb	P	Si	Zn	Al
Pure Cu	99.983	0.000	0.000	0.013	0.003	0.001	0.000
Cu-0.26Sn	99.502	0.257	0.006	0.130	0.102	0.002	0.001
Cu-0.57Sn	99.139	0.574	0.009	0.166	0.107	0.003	0.002

2.2 Preparation of the test specimen

The heat treatment process begins with homogenization at 500°C for 12h and next solution treatment at 750°C for a 2h soaking period. During the soaking period, the specimen can fully homogenize. Once the soaking period has ended, the specimen was quenched in a bath of salt ice water. Quenching was continued until the specimen reached ambient temperature. For the cold rolling process, these samples were machined to dimensions of 3.75 x 16 x 300, 5 x 16 x 300, 7.5 x 16 x 300, and 15 x 16 x 300 in mm. A 10 HP rolling machine reduced 20%, 40%, 60%, and 80% of the solution heat-treated alloys, resulting the thickness finally 3.0 mm. Samples without deformation were identified as 0% cold rolled. These samples were then subjected to an hour of isochronal aging at various temperatures ranging from ambient temperature to 500°C at intervals of 50°C using a JSMF-30T electric muffle furnace with a capacity of 900± 3.0°C.

2.3 Collecting test data

2.3.1 Tensile testing

Tensile testing was conducted at ambient temperature with the help of an Instron testing apparatus. The sample was prepared with a 3 mm thickness and 10 mm width, adjusting the gauge length to 25 mm and width to 6 mm, while applying a strain rate of $10^{-3}s^{-1}$ during the procedure. Each condition was put through seven tests, all of which were conducted in compliance with ASTM guidelines. The genuine stress-strain curve is constructed using the value that most closely matches the average of the data.

2.3.2 Hardness measurement

The hardness of various thermal treated samples was evaluated using a Micro Vickers Hardness Tester, Mitutoyo HM-200. The tests employed a 100 g load and was applied for a dwell time of 20 seconds. For the microhardness measurements, three samples with surface dimensions of 15 x 15 mm with 3 mm thickness were prepared for individual measurement. Each aged specimen, polished with fine-grade emery paper, underwent over ten indentations at different locations on the surface.

2.3.3 Impact testing

The ASTM guidelines were followed when conducting the impact testing. Standard 10 x 10 x 55 mm specimens with 2 mm V-notch of 45°-angled, were used. For every test, the impact resistance of seven test pieces was assessed.

2.3.4 Microstructural characterization

Using a Versamet-II microscope, alloy specimens were being optically metallograph in the standard manner. After polishing with alumina, etchant for copper, a 1:1 mix of NH4OH and 3% H2O2 was applied. Fracture surfaces due to tensile loading, were subjected to SEM examination using the JEOL scanning electron microscope. Fig. 1 provides a detailed diagram illustrating every step of the process and testing involved.

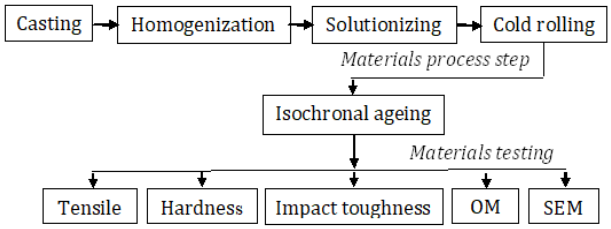

Fig. 1. Steps of material processing and testing.

3. RESULTS

3.1 Tensile properties

Tensile tests are conducted at the beginning for various cold deformed samples, including pure copper and two copper-tin alloys. The first alloy contains 0.26% tin, and the second has 0.57% tin. Figs. 2 and 3 illustrate the changes in UTS as well as the corresponding elongation percentages of these experimental alloys. The graph shows that sample strength increases with deformation, and the addition of trace elements usually leads to a higher rate (Fig. 2). Furthermore, a higher concentration of Sn correlates with increased tensile strength. More specifically, copper exhibits a strength of 307 MPa when it is cast or undergoes 0% cold rolling, which increases to 316 MPa when alloyed with 0.26% tin. Adding 57% tin further raises its strength to 332 MPa, while applying 80% cold rolling results in strength values of 350, 358, and 395 MPa.

With respect to percent elongation measurements, the accompanying figure shows a clear trend: as the degree of deformation applied to the specimen increases, the proportion of the original length that the specimen can elongate, i.e., the percent elongation, tends to decrease. The percentage of elongation values has been altered as follows: for copper, it decreased from 14.0% to 9.5%; for the first alloy, it dropped from 13.0% to 8.8%; and for the second alloy, it declined from 12.0% to 7.5%. This observation implies an opposite trend to a simple, linear elongation expectation, where more deformation would correspond to proportionally more elongation. In Fig. 3, this inverse relationship is illustrated, highlighting that higher deformation levels correspond to a smaller relative elongation of the sample.

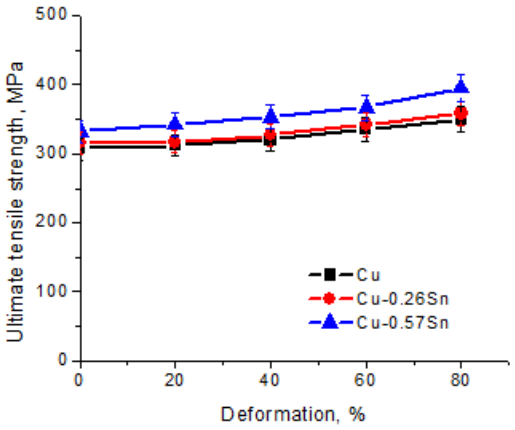

Fig. 2. Fluctuations of average ultimate tensile strength of the alloy samples during cold rolling.

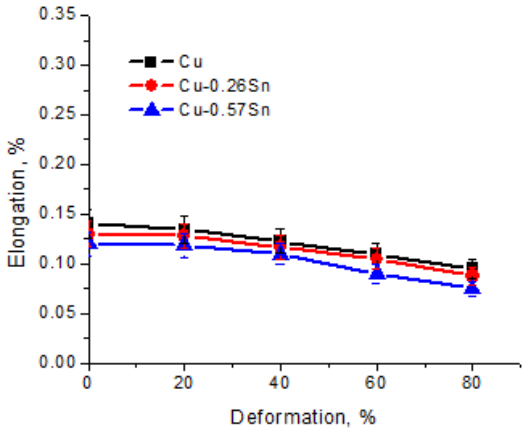

Fig. 3. Fluctuations of average elongation percentages of the alloy samples during cold rolling.

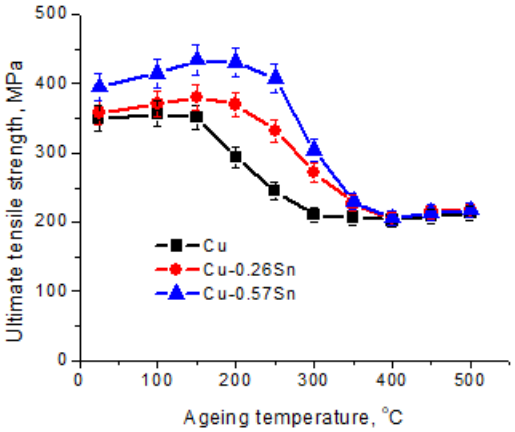

Fig. 4. Average ultimate tensile strength changes with ageing temperature when aged isochronally for one hour.

Fig. 4 illustrates the average test results for the ultimate tensile strength of eighty percent of cold-rolled samples, which includes two additional Sn-doped Cu alloys and commercially pure Cu. Except for Cu, the outcomes of the

isochronal aging treatment lasting one hour suggest that the other two samples achieve a certain level of strength during the initial phases of aging. More precisely, copper exhibits 294 MPa strength when aged at 200°C at the peak aged condition, but 0.26 and 0.57 Sn-doped copper exhibit 370 and 431 MPa, respectively. A significant decline in strength is noted at higher aging treatments, specifically beyond 200°C. Furthermore, there is no discernible difference between them in strength observed beyond a temperature of 350°C.

To address the concerns related to tensile behavior and the effects of aging, the true stress-strain plots obtained are illustrated in Fig. 5. Aged at 200°C and 450ºC for an hour are referred to as under-aged, peak-aged, and over-aged states, respectively, in the absence of aging treatment. The curves corresponding to various samples show some variation between the tensile strength and the slope of the actual stress-strain curves in the absence of any ageing treatment (Fig. 5a). Stress levels are lowest for commercially pure Cu, higher for lower Sn-doped alloys, and highest for greater Sn-doped alloys.

The graph's slopes drop as shown in the under-aged condition after an hour of aging at 200°C, which is regarded as the peak aged condition (Fig. 5b). Furthermore, the alloy with additional Sn added reduces more and the elongation drops little. The stress-strain curves' slope increases as the alloys age at 450°C for an hour, reaching over-aged conditions (Fig. 5c). Additionally, the samples' elongation significantly rises.

The average Young's modulus values of three samples under the previously indicated aging regime are shown in Fig. 6. The Young's modulus of the Sn-added alloys slightly increases under without ageing condition. With the exception of the base material Cu, all alloys reach a certain magnitude at their peak aged conditions. Likewise, under excessive aging treatment, alloys exhibit increased elongation and decreased strength, leading to a significant decrease in modulus.

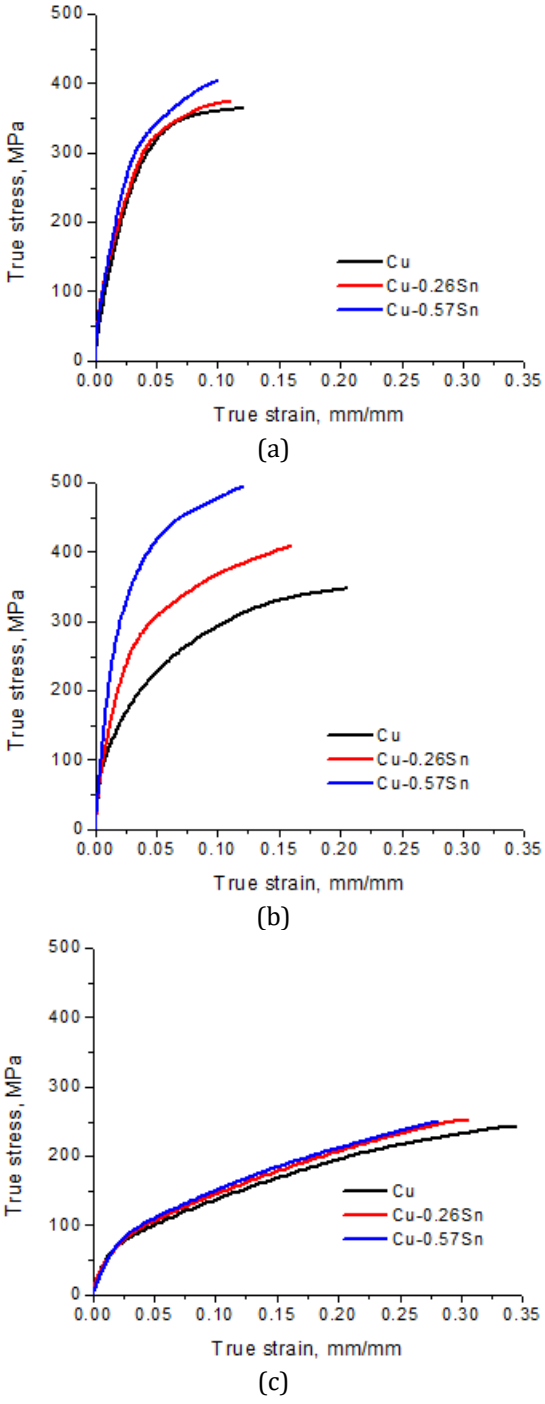

Fig. 5. True stress-true strain curves of the alloy samples (a) without ageing treatment, (b) aged at 200°C and (c) 450°C for 1h.

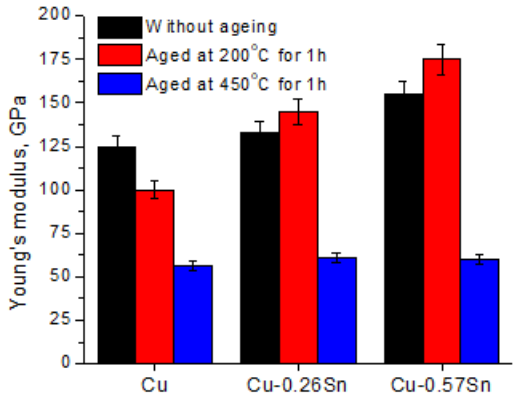

Fig. 6. Changes in the samples' Young's modulus as they aged.

3.2. Microhardness

Again, the microhardness of three samples under those aging conditions is measured, and average values are show in Fig. 7. The hardness result of the samples completely obeys the tensile behavior observed during the aging process. When compared to pure copper, modest added alloys usually show higher hardness ratings. Element-added alloys exhibit some hardness improvement in the peak aged condition. At the overaged condition, all the samples drastically lose their hardness.

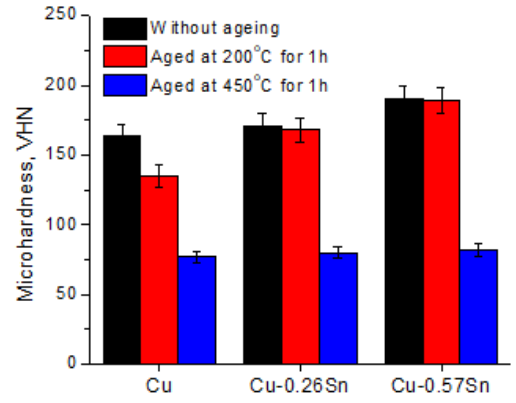

Fig. 7. Variations in micro hardness of the samples in different ageing state.

3.3. Impact toughness

Fig. 8 presents a bar graph illustrating the experimental average impact values obtained for the tested materials. It is evident that the two alloyed samples, excluding the pure Cu reference, exhibit diminished impact strength attributable to the addition of alloying elements in small quantities. This reduction becomes particularly acute at the peak aged condition, where a significant drop in impact energy is recorded. Furthermore, the progression into over-aging further exacerbates this phenomenon, leading to a more substantial loss of impact energy compared to the peak aged state.

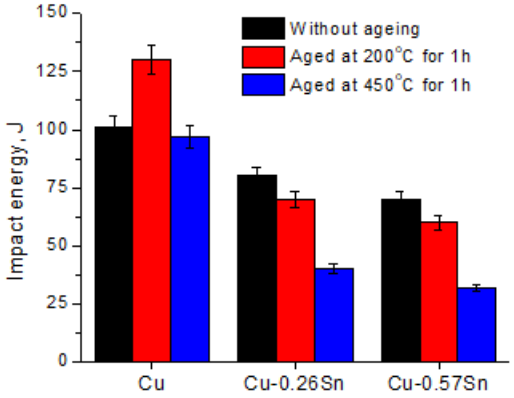

Fig. 8. Changes in the impact energy of the samples in different ageing state.

3.4. Optical micrographs

After solution treatment, 80% plastic deformation, and ageing at 200 °C for 60 min, the microstructure of pure copper (Fig. 9a) shows relatively thin grain boundaries. In contrast, the tin-doped alloys (Figs. 9b and 9c) exhibit noticeably denser grain boundaries, and the density increases with tin content (0.26% and 0.57% Sn). Furthermore, after severe cold rolling, heterogeneous grains exhibit non-uniform distribution and are dispersed throughout the microstructure.

3.5. Fractography

SEM analysis was employed to examine how different levels of Sn affect the fracture characteristics of pure Cu. The investigation involved conducting a tensile test on alloy samples at a strain rate of 10-3s-1 that had undergone 80% cold rolling and subsequent aging at 200°C for one hour. The resulting fracture surface was then analyzed, as depicted in Fig. 10. The tensile fracture mechanism of severely deformed Cu involves combined trans-granular and intergranular ductile fracture (Fig. 10a). Sn-doped alloys have deep equiaxed volume and fewer dimples. There are also some flat, smooth patches with bright ridges scattered throughout. In contrast, Sn addition shows a deeper depression due to its larger atomic size than copper (Fig. 10b). As the Sn concentration

increases, this tendency becomes more pronounced and causes precipitation from the alloy's grain boundaries as well as the emergence of several micron-scale phases that are rich, hard, and brittle (Fig. 10c).

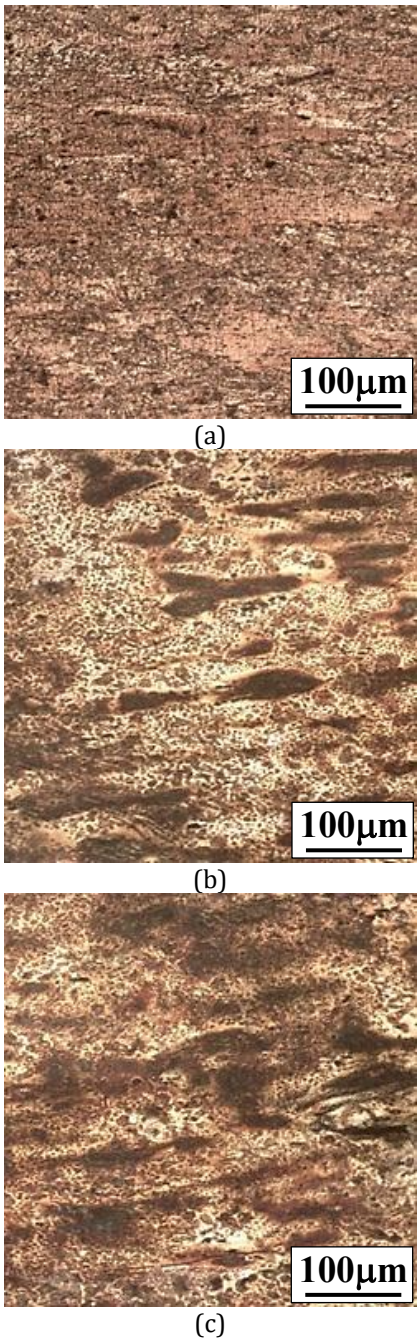

(a)
(b)
(c)

Fig. 9. Optical microstructure of eighty percent deformed (a) Cu, (b) tin-doped Cu-0.26Sn and (c) Cu-0.57Sn alloy with solution-treated and aged for 1h at 200°C.

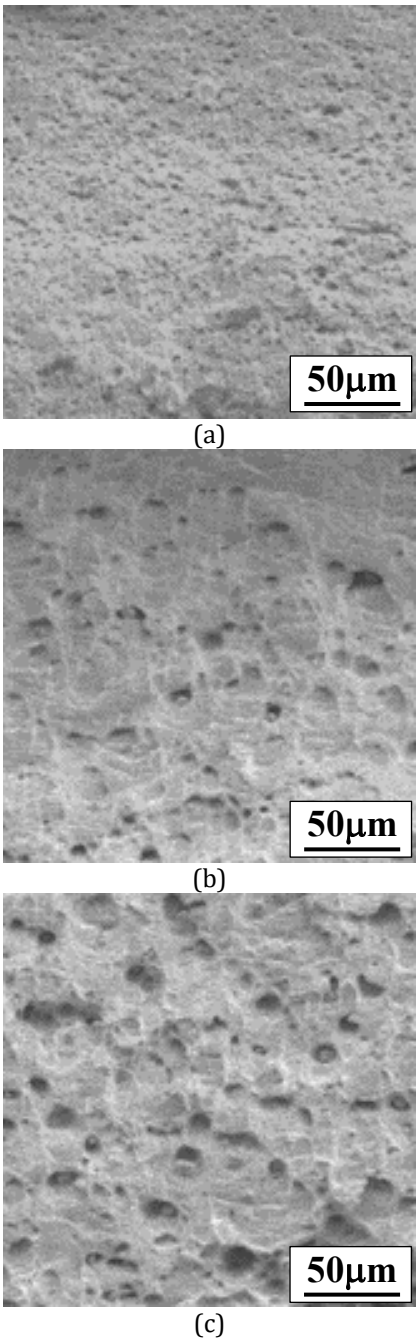

(a)
(b)
(c)

Fig. 10. SEM fractography due to tensile test of the aged samples (a) Cu, (b) tin-doped Cu-0.26Sn and (c) Cu-0.57Sn alloy.

4. DISCUSSION

According to tensile test results, the extent of the deformation enhances the average strength of the samples, and the addition of trace elements typically occurs at an elevated rate (Fig. 2). One explanation for this phenomenon is that the grain size diminishes with cold rolling, while the grain boundary density increases as the rolling reduction intensifies. Smaller grain sizes are more effective in hindering the movement and

multiplication of dislocations. Due to the differing BCC crystal structure of Sn that precipitates within the FCC Cu matrix, Sn demonstrates a greater tensile strength. The increased tensile strain may be a consequence of the coherency strain induced by β-Sn precipitates. A higher Sn content in the alloy, which forms a complex structure distinct from that of Cu, may explain the accelerated increase in tensile strength associated with cold rolling.

The material developed defects due to subgrain boundaries and a greater dislocation density during excessive strain. Both are unfavorable for the elongation of any material. Additionally, it demonstrates that the elongation of Cu is somewhat greater compared to alloys including trace additions (Fig. 3). The lattice is distorted by solid solution strengthening, which also offers resistance against dislocation motion. As usual, the decrease in ductility is accelerated by higher levels of Sn addition. [13].

In this particular situation regarding the effects of aging, materials typically lose strength as a result of stress relief, as pure copper demonstrated (Fig. 4). However, the formation of distinct precipitates in Sn-doped alloys results in an increase in strength. Precipitation formation and stress relevancy are the two events that occurred here. In this case, strengthening outweighs softening, leading to increased strength. Because of the over-aging impact, which includes stress release, dislocation rearrangement, recovery, and grain development in the samples, strength loss is more noticeable at higher aging temperatures [13]. As the recovery process proceeds, the subgrains spin and adopt a new orientation while the distorted grains soften. Around 350°C, recrystallization becomes more complete as it ages.

Without ageing treatment, it has been shown that as the Sn content rises, so does the amount of solid-soluble Sn in the α-phase alloy (Fig. 5). This creates a lattice distortion stress field that effectively prevents dislocation movement, increasing the tensile strength but decreasing the alloy's elongation. Additionally, coherency strain may have been created by the different crystal orientation between Sn and Cu matrix as well as β-Sn precipitates, resulting in increased strength in this alloy [14, 15]. The dislocation theory provides an explanation for the peak aged state occurrence. Sn creates the crystal structure of the stable primary intermediate phases Cu3Sn, Cu41Sn11, Cu10Sn3, and Cu6Sn5 as well as the terminal solid solution phases α-Cu and β-Sn during solidification and aging [14]. The amount of Sn added to the alloys determines the degree of these intermetallics. However, the two most significant intermetallic compounds that perform exceptionally well are Cu3Sn and Cu6Sn5. Additionally, Sn produces intermetallics via the casting environment, with trace contaminants. Tensile strength is strengthened as a result of the limited quantity of fine precipitates preventing dislocation movement. Ductility minima are a reflection of these precipitation episodes. A combination of these effects decreases the slope of the curve. In the state of over-aging, these results from recovery, precipitation coarsening, and dislocation rearrangement of the alloys. dispersed fine precipitates to create coarse precipitates, which become less resistant and prevent dislocation movement [16, 17]. All alloys have clearly greater elongation as a result.

The element-added alloys exhibit a modest rise in Young's modulus, as is typical due to solute solution strengthening under aged circumstances (Fig. 6). Young's modulus somewhat decreases as pure copper ages because it loses some of its strength. In some alloys, certain precipitates occur that block the dislocation movement, reducing elongation and increasing tensile strength. As a result, a percentage of these values, the Young's modulus, increases in an increasing direction. As is common, Sn-doped alloys show greater values for a higher degree of intermetallic formation. Coarse precipitates are not more successful than fine ones at providing sufficient stiffness to prevent dislocation movement, and high ageing temperatures cause the dislocations to reorganize into the alloy through recovery and recrystallization [13].

Minor added alloys demonstrate greater hardness, attributed to solid solution strengthening and distinct intermetallic formation with copper (Fig. 7). Compared to both similar lattices, the FCC and BCC lattice alloys show distinct supersaturated solid solution patterns with greater internal stress. In this instance, the cold rolling also starts the complicated structure to form. It should be noticed that Sn has a larger atomic size than Cu. Consequently, the internal tension is accelerated

when Sn is added to the Cu matrix. Therefore, the highest hardness is maintained by excellent impacted alloy. It can be explained that the alloy's strengthening is greatly aided by the various intermetallic formation with impurities during casting. Such a nature is seen because these intermetallics prevent dislocation movement under aging treatment [18]. The strain energy linked to different lattice imperfections, such dislocations and vacancies, is greatly increased as a result of intensive cold working, improving hardness. A number of significant processes, such as stress relief, dislocation rearrangement, recovery, recrystallization, and grain formation, take place when they are exposed to higher temperatures throughout the aging process. The number of dislocations decreases as a result of this temperature-induced atomic migration within the crystal lattice, which eventually results in a change in hardness. The subgrains spin and adopt a new orientation as the recovery process advances, and the damaged grains soften. It is crucial to recognize that annealing involves recrystallization, in which heating cold-worked samples produces new, stress-free crystals [19].

Two samples containing a minor amount of alloying exhibit reduced impact strength due to solid solution strengthening (Fig. 8). In the peak aged condition, a significant drop in impact energy can be connected to the development of different precipitates as previously discussed. The minima in ductility reflect these precipitation sequences. The early nucleation sites found in fine precipitates act as the source of micro-voids. Consequently, the fracture resistance of the material is diminished. Additionally, this "pinning" effect caused by the precipitate particles also leads to a reduction in total elongation. The increased formation of intermetallic compounds with Sn results in a more vigorous reaction. Under over ageing conditions, which involve microstructural changes such as equiaxed grain formation and precipitation coarsening similar to cast alloys, there is a more significant reduction in energy observed. Large brittle intermetallic phase particles can adversely affect impact properties as they serve as initiators of cracks. [20].

The diverse grains that are scattered in the rolling directions constitute the complete microstructure (Fig. 9). Extensive plastic deformation destroys the grain boundaries, resulting in the sub-grains formation. The slight addition causes some variations because the minimum and maximum Sn-doped alloys have relatively thin grain boundaries, followed by Cu. During solution treatment, there are fewer intermetallics in both amount and size because copper materials have the fewest impurities, such as Fe, C, P, etc. Because the supersaturated solid solution patterns of alloys containing the FCC Cu and BCC Sn lattices differ, tin forms denser grain boundaries. Furthermore, Sn has a larger atomic size than Cu, it tends to allocate to grain boundaries, giving alloys containing Sn denser grain boundaries. An elevated Sn content causes the alloy's grain boundary to be dense [15].

Fracture failure is primarily caused by small second-phase particles within the grains and boundaries, which facilitate microcrack initiation and propagation (Fig. 10). The presence of numerous dimples indicates ductile fracture. Sn-doped alloys exhibit fewer deep equiaxed dimples and flat areas interspersed with bright ridges due to fractures initiated at thicker grain boundaries. The larger atomic size of Sn compared to copper leads to deeper dimples, with increased Sn content resulting in more brittle, hard phases appearing on a microscopic scale and emerging from the grain boundaries of the alloy [14].

5. CONCLUSION

Ageing studies on severe deformed copper and different tin-doped from lead-free solder showed that:

Recycled copper typically includes 0.26% to 0.57% tin, depending on the cleaning method, after scraped copper was used to remove the main solder connection and cleaned with wire brushing.

Trace Sn boosts copper strength by raising solid-soluble Sn in the α-phase matrix, distorting the lattice and hampering dislocation movement, leading to enhanced tensile strength but reduced elongation. Coherency strain from BCC Sn and β-Sn precipitates in FCC Cu generates varying crystal orientations, further bolstering the alloy's strength.

During casting and thermal treatment, Sn interacts with Cu and impurities, forming

precipitates that impede dislocation movement, boosting tensile strength. These precipitation sequences limit ductility, and higher aging temperatures decrease alloy strength from over ageing effects.

Alloys aged at higher temperatures show a steeper slope in stress-strain curves near over-aging, when fine precipitates merge into larger ones, reducing their ability to hinder dislocation motion and allowing for increased elongation in all alloys.

Commercially pure copper consists of negligible amounts of intermetallic compounds at the grain boundaries, while tin forms a range of intermetallic compounds and has a larger atomic size than copper.

Heavily deformed Cu fractures via intergranular and trans-granular ductile mechanisms due to trace second-phase particles. These particles are present in the material's grains and along its edges, and they aid in the development of microcracks. Since Sn has a larger atomic size and several brittles, hard, and rich phases at the grain boundaries of the alloys, it exhibits fracture failure in the early hours due to the deeper dimple.

Acknowledgement

This study is an integral component of the approved research project as well as supported by the Miyan Research Institute of IUBAT, Dhaka.

REFERENCES

[1] U. Prahl, A. Zilly and J. Dölling, "Advances in Copper, Copper Alloys and Their Processing," Metals, vol. 15, no. 4, pp. 2075-4710, 2025, doi: 10.3390/met15040375.

[2] L. Collini, "Copper Alloys – Early Applications and Current Performance – Enhancing Processes," InTech, Rijeka, Croatia, 2012.

[3] O. S. Novikova, A. E. Kostina, Y. A. Salamatov, D. A. Zgibnev, and A. Y. Volkov, "The influence of defor-mation at cryogenic or room temperature followed by annealing on the structure and properties of copper and its Cu–3Pd and Cu–3Pd–3Ag (at. %) alloys," Frontier Materials & Technologies, no. 2. pp. 67-74. 2023, doi: 10.18323/2782-4039-2023-2-64-6.

[4] M. N. Islam, R. A. Shijan, M. Motalab and M. R. A. R. Rafi, "Analysis of mechanical properties in lead-free solders subjected to flash aging. Materials Advances, vol. 7, no. 4, pp. 2322–2336, 2026, doi: 10.1039/D5MA01436K.

[5] M. Zhao, L. Zhang, Z. Q. Liu, M. Y. Xiong and L. Sun, "Structure and properties of Sn-Cu lead-free solders in electronics packaging," Science and Technology of Advanced Materials, vol. 20, no. 1, pp. 421-44, 2019, doi: 10.1080/14686996.2019.1591168.

[6] M. M. Rahman, S. R. Ahmed and M. S. Kaiser, "On the Investigation of Reuse Potential of SnPb-Solder Affected Copper Subjected to Work-Hardening and Thermal Ageing," Materials Characterization, vol. 172, pp. 1-19, 2021. doi: 10.1016/j.matchar.2021.110878.

[7] M. S. Kaiser, "Impact of trace amounts of Sc and Zr on the tribological performance of Al-Bronze against stainless steel counterface in varying conditions," Engineering Transactions, vol. 72, no. 3, pp. 263-284, 2024, doi: 10.24423/EngTrans.3281.2024.

[8] C. Zeng, B. Zhang, A. H. Ettefagh, H. Wen, H. Yao, W. J., Meng and S. Guo, "Mechanical, thermal, and corrosion properties of Cu-10Sn alloy prepared by laser-powder-bed-fusion additive manufacturing, Additive Manufacturing, vol. 35, pp. 1-8. 2020, doi: 10.1016/j.addma.2020.101411.

[9] B. Liu et al., "Effects of Al addition on corrosion behavior and mechanical property of high-strength and high-elasticity Cu-20Ni-20Mn-0.3Nb-0.3Cr-0.3Zr alloy," Materials Characterization, vol. 167, p. 110476, 2020, doi: 10.1016/j.matchar.2020.110476.

[10] K. H. Kazmi, S. K. Sharma, A. K. Das, A. Mandal and A. Shukla, "Development of Wire Arc Additive Manufactured Cu-Si Alloy: Study of Microstructure and Wear Behavior," Journal of Materials Engineering and Performance, vol. 33, pp. 110-119. 2024, doi: 10.1007/s11665-023-07972-9.

[11] J. Ge, H. Shi, Z. Li, S. Xu, Y. Zheng, W. Jiang, A. Meng, Y. Zhao, J. Li and G. Wang, "Mechanical properties and deformation mechanism of Cu–Ni–Al ternary alloys with different coherent precipitation characteristics," Journal of Materials Science, vol. 61, pp. 9796–9812, 2026, doi: 10.1007/s10853-026-12481-w.

[12] A. M. Gnusina and A. V. Svyatkin, "The influence of phosphorus microalloying on the structure formation of CuZn32Mn3Al2FeNi multicomponent brass," Frontier Materials & Technologies, no. 3, pp. 31–40, 2024, doi: 10.18323/2782-4039-2024-3-69-3.

[13] M. M., Rahman and S. R. Ahmed, "Effects of work-hardening and post thermal-treatment on tensile behaviour of solder-affected copper," Pro. of the Institution of Mechanical Engineers, Part L: Journal of Materials: Design and Applications, vol. 237, no. 5, pp. 981-1005, 2023, doi: 10.1177/14644207221131878.

[14] A. Leineweber, "The Cu–Sn System: A Comprehensive Review of the Crystal Structures of its Stable and Metastable Phases," Journal of Phase Equilibria and Diffusion, vol. 44, pp. 343-393, 2023, doi: 10.1007/s11669-023-01041-3.

[15] J. Peng, J. Li, B. Liu, Q. Fang and P. K. Liaw, "Origin of thermal deformation induced crystallization and microstructure formation in additive manufactured FCC, BCC, HCP metals and its alloys," International Journal of Plasticity, vol. 172, pp. 1-21. 2024, doi: 10.1016/j.ijplas.2023.103831.

[16] P. Yang, D. He, W. Shao, Z. Tan, X. Guo, S. Lu and K. Anton, "Study of the microstructure and mechanical properties of Cu–Sn alloys formed by selective laser melting with different Sn contents," Journal of Materials Research and Technology, vol. 24, pp. 5476-5485, 2023, doi: 10.1016/j.jmrt.2023.04.198.

[17] A. Ahmed, N. Iqbal, M. S. Kaiser and S. R. Ahmed, "Thermo-mechanical and optical characteristics of cold-rolled copper with natural melting impurities. AIP Conference Proceedings, vol. 2324, no. 1, pp. 0300171-7, 2021, doi: 10.1063/5.0037516.

[18] G. Xu, Y. Zhu, L. Peng, H. Xie, Z. Li, S. Huang, Z. Yang, W. Zhang, and X. Mi, "Effect of Sn Addition on Microstructure, Aging Properties and Softening Resistance of Cu-Cr Alloy," Materials, vol. 27, no. 15, pp. 1-9, 2022, doi: 10.3390/ma15238441.

[19] H. Wang, P. Y. Yang, W. J. Zhao, S. H. Ma, J. H. Hou, Q. F. He, C. L Wu, H. A. Chen, Q. Wang, Q. Cheng, B. S. Guo, J. C. Qiao, W. J. Lu, S. J. Zhao, X. D. Xu, C. T. Liu, Y. Liu, C. W. Pao and Y. Yang, "Lattice distortion enabling enhanced strength and plasticity in high entropy intermetallic alloy," Nature Communications, vol. 15, no. 6782, pp. 1-10, 2024, doi: 10.1038/s41467-024-51204-0.

[20] K. Manu, J. Jezierski, M. R. S. Ganesh, K. V. Shankar, and S. A. Narayanan, "Titanium in Cast Cu-Sn Alloys-A Review, "Materials, vol. 14, no. 16, pp. 1-36, 2021, doi: 10.3390/ma14164587.